Journal of Power Sources 195 (2010) 8104–8109

Contents lists available at ScienceDirect

Journal of Power Sources

journal homepage: www.elsevier.com/locate/jpowsour

Effective thermal conductivity and thermal contact resistance of gas diffusion layers in proton exchange membrane fuel cells. Part 2: Hysteresis effect under cyclic compressive load

E. Sadeghi[a,b,*], N. Djilali[a], M. Bahrami[b]

[a] Dept. Mechanical Eng., and Institute for Integrated Energy Systems, University of Victoria, P.O. Box 3055, Victoria, BC, Canada V8W 3P6
[b] Mechatronic Systems Engineering, School of Engineering Science, Simon Fraser University, Surrey, BC, Canada V3T 0A3

ARTICLE INFO

Article history:
Received 15 July 2010
Accepted 19 July 2010
Available online 22 July 2010

Keywords:
Hysteresis
Cyclic compression
TCR
Effective thermal conductivity
Heat transfer

ABSTRACT

Heat transfer through the gas diffusion layer (GDL) is a key process in the design and operation of a PEM fuel cell. The analysis of this process requires the determination of the effective thermal conductivity as well as the thermal contact resistance between the GDL and adjacent surfaces/layers. The Part 1 companion paper describes an experimental procedure and a test bed devised to allow separation of the effective thermal conductivity and thermal contact resistance, and presents measurements under a range of static compressive loads. In practice, during operation of a fuel cell stack, the compressive load on the GDL changes.

In the present study, experiments are performed on Toray carbon papers with 78% porosity and 5% PTFE under a *cyclic* compressive load. Results show a significant hysteresis in the loading and unloading cycle data for total thermal resistance, thermal contact resistance (TCR), effective thermal conductivity, thickness, and porosity. It is found that after 5 loading-unloading cycles, the geometrical, mechanical, and thermal parameters reach a "steady-state" condition and remain unchanged. A key finding of this study is that the TCR is the dominant component of the GDL total thermal resistance with a significant hysteresis resulting in up to a 34% difference between the loading and unloading cycle data. This work aims to clarify the impact of unsteady/cyclic compression on the thermal and structural properties of GDLs and provides new insights on the importance of TCR which is a critical interfacial transport phenomenon.

1. Introduction

Commercialization of PEM fuel cells requires further progress in improving operational lifetime [1]. A number of degradation mechanisms need to be better understood, including those associated with the deterioration of the gas diffusion layer (GDL) due to mechanical stresses. In the companion paper [2] the effects of *constant* compressive loads representative of the clamping of a stack were investigated for GDLs. In practice, the GDL as well as other components, including the membrane and catalyst layer, will be subjected to additional hygro-thermal stresses that arise due to varying temperature and relative humidity during operation, and that are *cyclic* in nature. These stresses induce material degradation and compromise performance and lifetime [3,4]. The variation in the compressive load affects all the transport phenomena and consequently the performance of the entire system. In addition, servicing and/or reconditioning that involves unclamping and opening of a stack may be required on a number of occasions over the course of the operational lifetime of the stack, resulting in another type of cyclic compression. The effects of cyclic compression on the fuel cell components need to be examined and better understood.

The focus in this study is on the GDL which provides five key functions in a PEM fuel cell: (1) mechanical support, (2) electronic conductivity, (3) heat removal, (4) reactant access to catalyst layers, and (5) product removal [5]. Thus, accurate knowledge of the mechanical and thermal characteristics of GDLs under different compressive loads is required to determine related transport phenomena such as water and species transport, reaction kinetics, and the rate of phase change.

Several studies are available on the effects of steady-state compression on fuel cell components and performance; however, the effects of cyclic compression have not been studied in-depth. Rama et al. [1] presented a review of the causes and effects of performance degradation and failure in various components of PEM fuel cells. They reported that over-compression and inhomogeneous compression of GDLs induced during stack assembly or during operation reduce the porosity, hydrophobicity, and gas permeabil-

* Corresponding author at: Dept. Mechanical Eng., and Institute for Integrated Energy Systems, University of Victoria, P.O. Box 3055, Victoria, BC, Canada V8W 3P6. Tel.: +1 7787828587; fax: +1 2507216051.
E-mail address: ehsans@uvic.ca (E. Sadeghi).

0378-7753/$ – see front matter © 2010 Elsevier B.V. All rights reserved.
doi:10.1016/j.jpowsour.2010.07.051

ity. This increases the tendency for flooding in GDLs, which results in an increase in mass transport losses.

Kleemann et al. [6] investigated the local compression distribution in the GDL and the associated effect on material electrical resistance and electrical contact resistance. They also measured the mechanical properties of fibrous paper and non-woven GDLs. The mechanical properties included Young's modulus, the shear modulus, and Poisson's ratio for in-plane and through-plane directions. They found that the combined value of the through-plane resistance and of the contact resistance with the microporous layer and catalyst layer is highly compression dependent and increases sharply at low compression pressures.

Escribano et al. [7] measured the thickness reduction of different types of GDLs including cloth, felt, and paper for the first and second loading over a range of compressive loads. They reported differences between the thickness data; the thickness values for the second loading were smaller and their variation over the range of compressions was smoother.

Zhou et al. [8] studied the effect of the clamping force on the electrical contact resistance and the porosity of the GDL using a finite element method. They assumed the GDL to be a porous elastic material and reported that after stack loading, the porosity was not uniform and that its minimum occurred in the middle of flow-field plate rib.

Bazylak et al. [9] used scanning electron microscopy (SEM) to investigate the effect of compression on the morphology of the GDL. They reported that the damage to the GDL is non-uniform under a small compression which was attributed to the surface roughness. However, as the compression pressure is increased, the damage was found to be more isotropic over the entire sample [9]. Bazylak et al. [9] experimentally showed that compressing the GDL causes a breakup of fibers and a deterioration of the PTFE coating.

Several studies used a guarded-hot-plate apparatus to measure the effective thermal conductivity and TCR of GDLs under different pressures [2,10–12]. Nitta et al. [10] argued that the effective thermal conductivity is independent of compression but Burheim et al. [11] reported that the effective thermal conductivity increases with compressive load; however, both studies showed that TCR, decreases with an increase in the compressive load. In the companion Part 1 of this study [2] we showed that the effective thermal conductivity increases with compression due to an increase in the number and size of contact spots. Khandelwal and Mench [12] investigated the effect of load cycling on the TCR between the GDL and an aluminum bronze material as well as the total resistance of the GDL by compressing the sample to 2 MPa and then releasing it for a single cycle. They found that the measured total resistance and TCR differed by 20% and 38%, respectively between the loading and unloading phases.

Although the studies available on the effect of compression-release on GDL properties are limited, numerous investigations have been performed in textile engineering that are relevant to the fibrous structure of GDLs. The first theoretical model in this field was proposed by van Wyk [13,14] in 1946 to explain the compression behavior of fiber assemblies with random orientations. van Wyk [13,14] assumed that the compression of a fibrous assembly increases the number of fiber–fiber contact points leading to individual fibers becoming bent between these contact points. He found a linear relationship between the pressure and the cube of the fiber volume fraction. van Wyk's relationship is a classical model in textile engineering, however, it does not account for fiber slippage and friction during compression. Also, it does not explain the non-recoverable strain during compression and the mechanical hysteresis during compression-release cycling. Recent studies [15–20] have focused on accounting for the fiber slippage and the hysteresis observed during compression-release cycling. The cycling induces energy dissipation as a result of viscous damping or

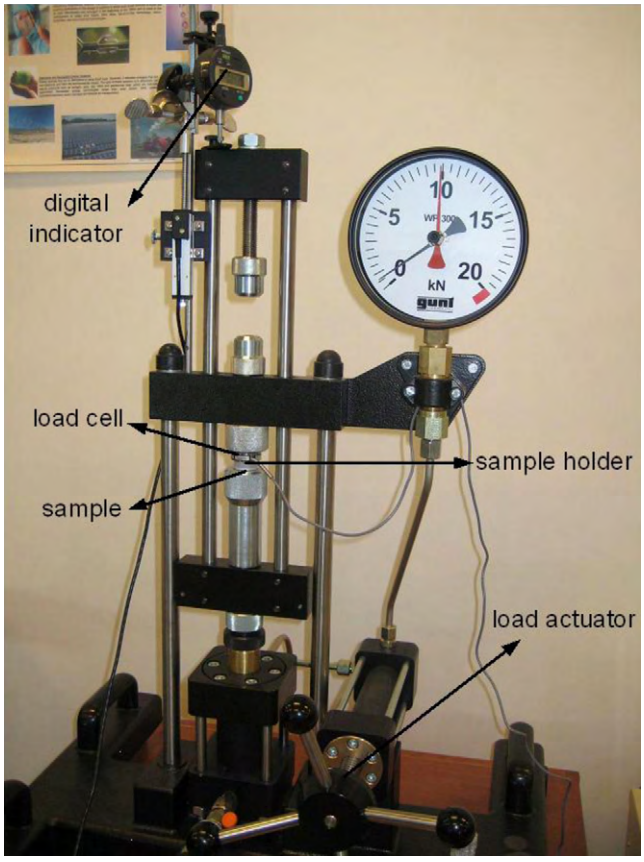

Fig. 1. Experimental apparatus used for thickness measurement.

frictional losses. An approach taken to model the hysteresis behavior of fibrous media is to consider the structure as a combination of series and parallel springs, dashpots, and Coulomb frictional element [15,16]. Dunlop [15] used such a model to perform simulation that yield a hysteresis loop with a shape similar to the experimental data, but no model verification was performed. Also, the viscoelastic nature of fibers was not considered. The compression hysteresis was theoretically modeled and verified against experimental data in [17–19] by applying the force, angular momentum, and bending equations to fiber assemblies. These models [17–19] reproduced the experimentally observed trends correctly but the values are different. Also, the hysteresis effect was independent of the number of load cycles as a result of neglecting the viscoelastic behavior of the fibers. Stankovic [20] measured the strain of different fabrics including hemp, cotton, viscous, and acrylic fabrics under compression-release cycles and observed a hysteresis in the stress–strain curve. He [20] reported that the hysteresis becomes smaller with repeated load cycling, and approaches zero at the 5th cycle.

Our literature review shows that the majority of the available studies have focused on the effect of steady-state compression on the structure and properties of GDLs; even though, cyclic compression occurs during the operation and lifecycle of a PEM fuel cell stack. The present study contributes to addressing this gap through a systematic investigation of the effects of cyclic compression on the GDL thermal and structural properties.

A test bed was designed and built to enable the measurement of thermal conductivity and TCR of porous media. The test bed was equipped with a loading mechanism that allows the application of various compressive loads on GDLs. Also, a tensile- compression apparatus is used to measure the thickness variation of GDLs under compression. Toray carbon papers with a porosity of 78% and

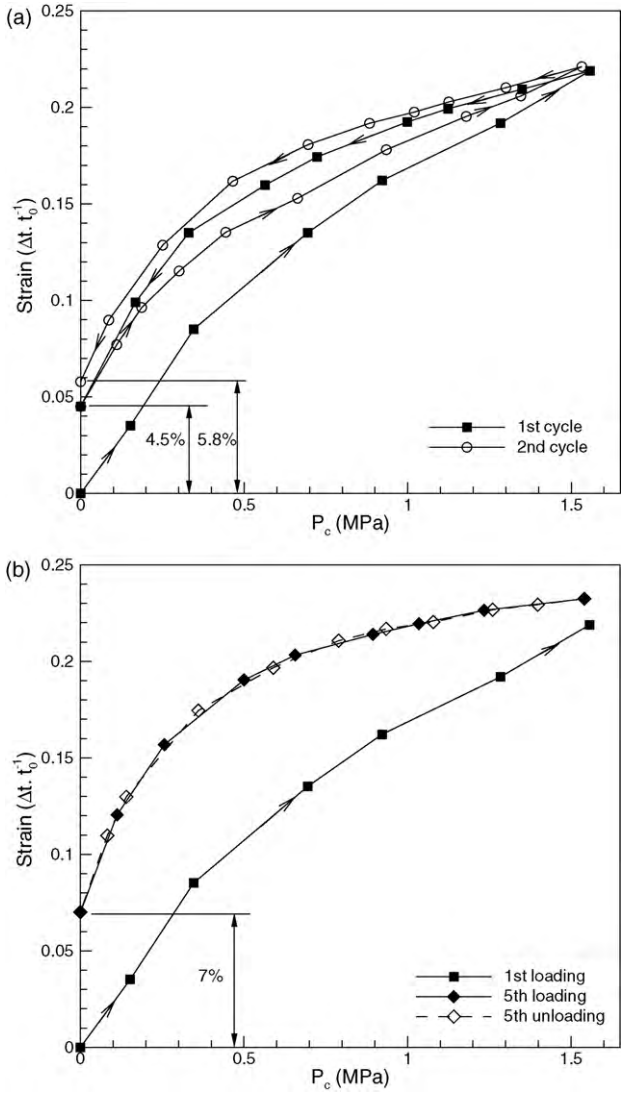

Fig. 2. Hysteresis in thickness variation of Toray carbon paper, 78% porosity and 5% PTFE, under cyclic compressive loads: (a) comparison of 1st and 2nd cycles; (b) comparison of 1st loading and 5th unloading.

5% PTFE content are used in the experiments. The effects of cyclic compression on the effective thermal conductivity, total thermal resistance, TCR, thickness and porosity of the GDL are investigated under vacuum condition. The load cycling in the experiments is continued until the loading and unloading data coincide. As we show later, this occurs at the 5th cycle for all properties. The compression-release curve of the thermal and structural properties is presented and the hysteresis observed in their behavior is explained.

2. Experimental study

The experimental apparatus for the thermal tests is a custom-made test bed designed for thermal conductivity and TCR measurements under vacuum and ambient pressure conditions and is described in detail in Part 1 [2]. Toray carbon paper TGP-H-120 with a porosity of 78%, 5% wet proofing, and an initial thickness of 0.37 mm was used in the mechanical and thermal experiments under cyclic compression. The apparatus used to monitor the sample thickness is shown in Fig. 1.

Thermal experiments were conducted under vacuum condition. A vacuum level of 10^{-5} mbar was achieved under the test

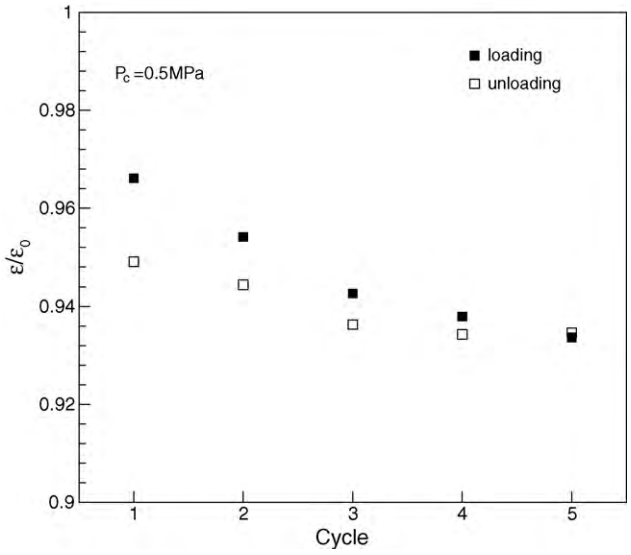

Fig. 3. Normalized porosity at different loading–unloading cycles, P_c = 0.5 MPa.

chamber using the vacuum machine. Cyclic compressive loads were applied to the sample continuously while simultaneously recording temperature and pressure at each load of the loading and unloading paths when steady-state conditions were achieved. The compression-release cycling was continued until no significant hysteresis effects were observed in loading-unloading curves; as discussed later, this happens at the 5th cycle.

The thickness of the GDL sample under the cyclic compressive load was measured separately using the tensile-compression apparatus shown in Fig. 1. The loading was stopped at the end of the 5th cycle when the difference between the loading and unloading paths became negligible. More details on the test procedure and data reduction of the thermal and mechanical experiments are provided in Part 1 of this study [2].

3. Results and discussion

Fig. 2 shows the thickness variation of the Toray carbon paper TGP-H-120 under cyclic compressive load. The thickness reduction is more significant at the beginning of the loading and as the pressure increases, the slope of thickness variation decreases. Since the micro-structure becomes more packed, its resistance to deformation under the load is higher. During unloading a number of deformed, slipped or broken fibers do not return to their original state; this results in a difference between the loading and unloading paths, creating the compression hysteresis. When the cyclic compression is repeated, the hysteresis effect becomes smaller, and the deformation reaches a steady-state. The variation in hysteresis may be a result of the viscoelastic behavior of the GDL fibers [16–20]. The difference between the unloaded and fresh samples is 4.5% for the first cycle. The difference gradually increases with each subsequent cycle, and reaches 7% at the 5th cycle and remains unchanged afterward. This result is consistent with the experimental data of Stankovic [20] which shows no change in the stress–strain curve after the 5th cycle for a variety of fabrics. The variation of the normalized porosity (i.e. the ratio of compressed to fresh GDL porosities) at different loading–unloading cycles is shown in Fig. 3 for a typical compressive load of 0.5 MPa. As shown, the porosity decreases as the number of cycles increases; this is a direct result of more permanent (irreversible) deformations in the micro-structure. We note that the difference between the porosity values of the loading and unloading paths decreases with continuing load cycling and becomes negligible at the 5th cycle.

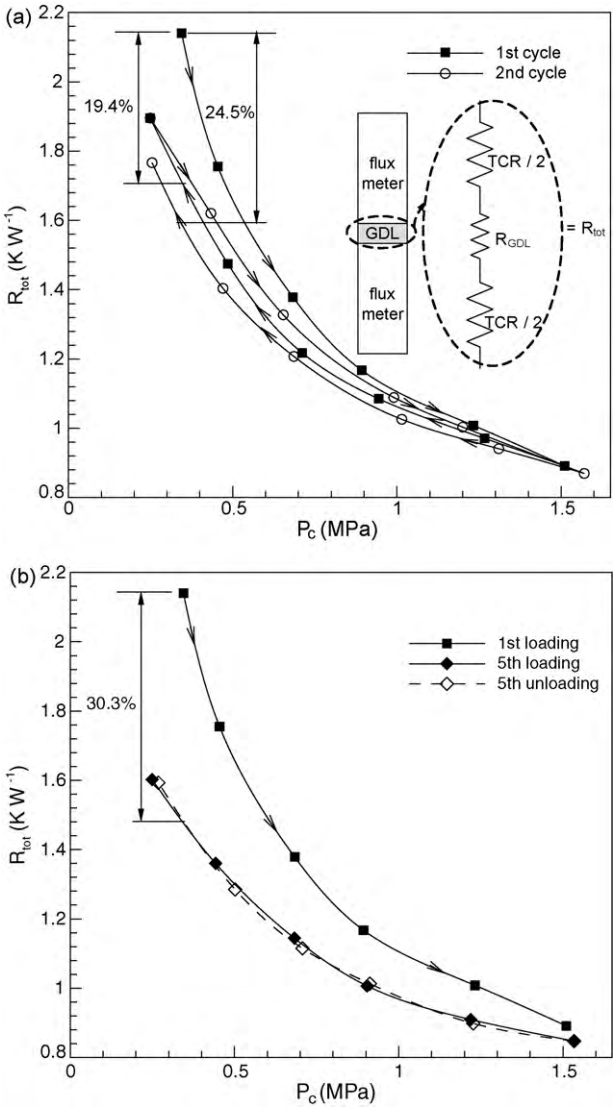

Fig. 4. Hysteresis in total thermal resistance under cyclic compressive load: (a) comparison of 1st and 2nd cycles; (b) comparison of 1st loading and 5th unloading.

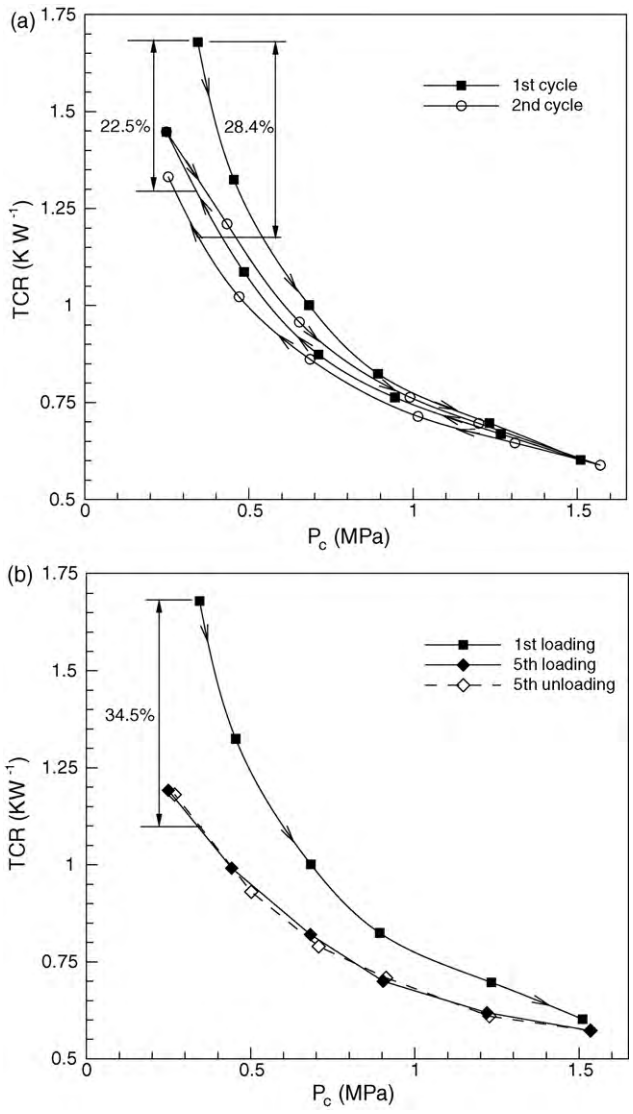

Fig. 5. Thermal contact resistance hysteresis under cyclic compressive load (a) comparison of 1st and 2nd cycles; (b) comparison of 1st loading and 5th unloading.

The impact of cyclic compressive load on the total thermal resistance of the GDL sample under vacuum condition is shown in Fig. 4. The total resistance decreases with an increase in compressive load due to the increased contact area between the GDL fibers as well as at the interface between the GDL and the fluxmeters surfaces. Increasing compression causes fiber breakage, irreversible deformations, and fiber slippage resulting in a hysteresis behavior in the total resistance of the unloaded structure. The hysteresis effect becomes gradually less important for the following cycles and eventually negligible at the 5th cycle. The hysteresis causes 19.4% and 24.5% differences in the total thermal resistance of the unloaded GDL sample with respect to the thermal resistance at the beginning of the loading process for the first and the second cycles, respectively, see Fig. 4. The hysteresis for the first cycle is consistent with the result of Khandelwal and Mench [12]. The thermal resistance hysteresis gradually increases and reaches 30.3% at the 5th cycle. A similar behavior is observed for the TCR variation under cyclic compression, which is shown in Fig. 5. However, the hysteresis seems to be higher for the TCR and starts at 22.5% at the first cycle, continues to 28.4% at the second cycle and reaches 34.5% at the end (5th cycle).

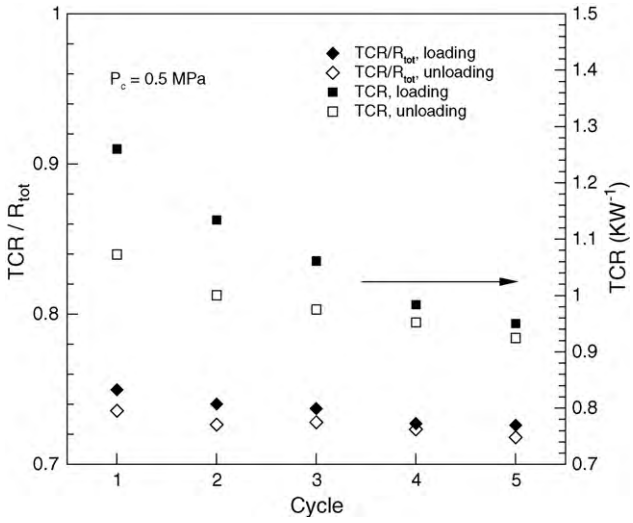

Fig. 6. TCR and "TCR to total resistance ratio" at different loading–unloading cycles, P_c = 0.5 MPa.

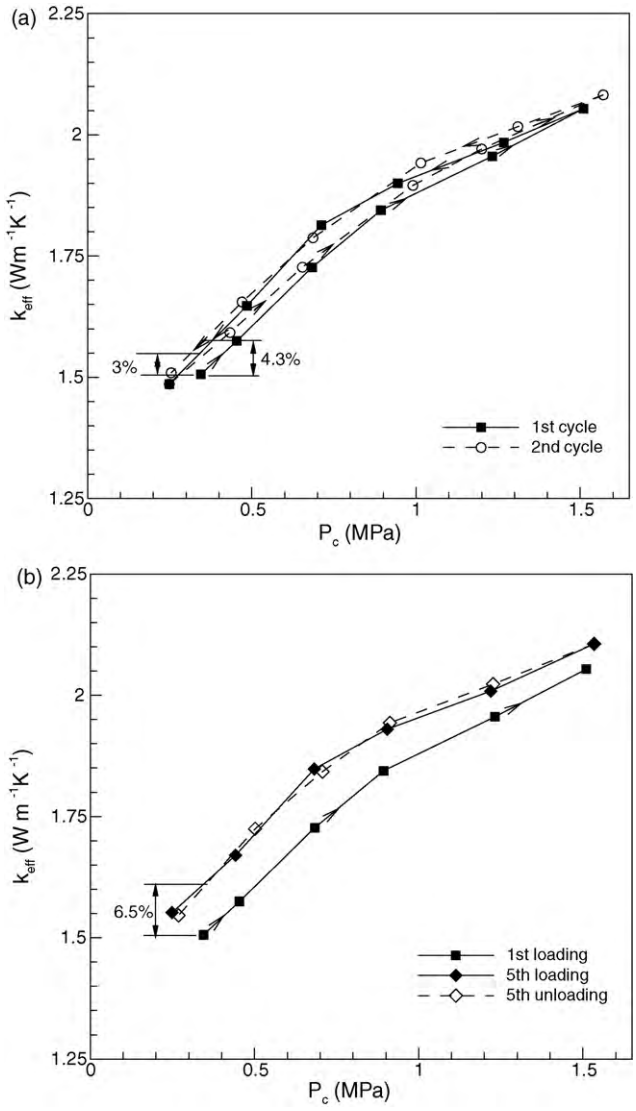

Fig. 7. Effect of loading and unloading on the GDL effective thermal conductivity: (a) comparison of 1st and 2nd cycles; (b) comparison of 1st loading and 5th unloading.

The variations of the TCR and "TCR to total resistance ratio" at different loading–unloading cycles are shown in Fig. 6 for a typical compressive load of 0.5 MPa. As expected, the TCR decreases as the number of loading cycles increases due to enhanced contact area at the GDL–solid (fluxmeter) interfaces. As the load cycling continues, the hysteresis in the TCR values decreases and becomes negligible for the 5th cycle. It should be noted that the "TCR to total resistance ratio" remains approximately constant during the loading–unloading cycles; it is also noteworthy that the TCR includes 73% of the total resistance of the sandwiched GDL. This clearly indicates the importance of TCR which remains the dominant resistance in the assembly even after several loading-unloading cycles. More importantly, the TCR to total resistance ratio remains almost constant; one can conclude that the loading-unloading cycles have an approximately equal impact (hysteresis effect) on both bulk resistance and TCR of GDLs. It should be emphasized that the TCR is an interface phenomenon and depends on the fibrous micro-structure (bulk GDL properties) and the solid surface characteristics as well as the compressive load; whereas the effective thermal conductivity is primarily a bulk property of a GDL. Consequently, any successful solution to reduce thermal resistance and/or improve thermal management of the membrane electrode

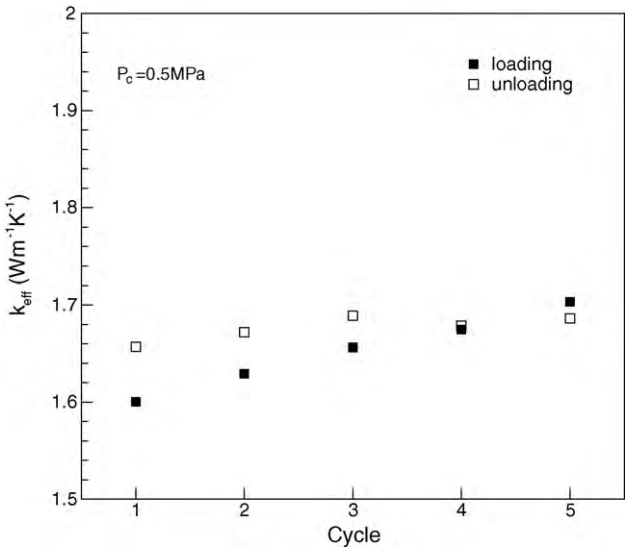

Fig. 8. Effective thermal conductivity at different loading–unloading cycles, P_c = 0.5 MPa.

assembly (MEA) should include interfacial phenomena such as the TCR, which to date have been largely overlooked.

Fig. 7 shows the effective thermal conductivity values at different contact pressures during the loading–unloading process. The effective conductivity increases with an increase in the compressive load due to larger contact areas between the contacting fibers providing a lower resistance path for heat flow [2]. Hysteresis is also observed in the thermal conductivity behavior as a result of the hysteresis in the total thermal resistance, TCR, and the sample thickness. The hysteresis in thermal contact resistance and TCR increases the thermal conductivity during unloading, whereas the mechanical hysteresis (reduction in thickness) has a reverse effect; the net effect is a smaller hysteresis in the effective thermal conductivity behavior in comparison with the TCR. This results in a maximum difference of 6.5% between the effective conductivity values of the unloaded GDL at the 5th cycle and the loaded GDL at the starting point.

The variation of the effective thermal conductivity of GDL under compression-release cycles is shown in Fig. 8 under vacuum condition for a typical compressive load of 0.5 MPa. The effective con-

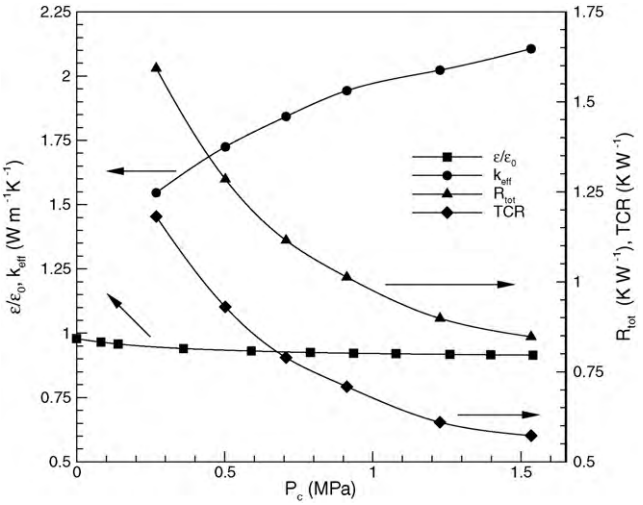

Fig. 9. Thermal and geometrical properties of Toray carbon paper TGP-H-120 with 5% wet proofing at quasi steady-state condition (after 5th loading cycle) under vacuum condition.

ductivity slowly increases with the number of loading cycles. Also, the thermal conductivity values during unloading are higher as a result of the irreversible deformations that occur during loading.

The results show that the thermal and geometrical properties of GDLs reach a quasi steady-state condition and remain unchanged after the 5th compression-release cycle. In practice, a fuel cell stack is subjected to many more than five loading–unloading cycles; therefore, the steady-state values for properties should be used in PEM fuel cell modeling. Fig. 9 summarizes the effective thermal conductivity, TCR, normalized porosity, and total thermal resistance (bulk and TCR) for the GDL sample used in this study over a range of compressive load.

4. Summary and conclusions

A test bed was designed and built to measure and predict thermal conductivity and thermal contact resistance of GDLs under cyclic compressive loads and vacuum condition. Toray carbon papers with 78% porosity and 5% PTFE were compressed from 0.25 MPa to approximately 1.5 MPa and then decompressed to the starting point to investigate the effects of cyclic compressive load. The number of load cycles was continued until hysteresis effects became negligible; this occurred at the 5th cycle. The thickness of the GDL was measured under cyclic compressive load using a tensile-compression machine. Results show a significant hysteresis in the total thermal resistance, TCR, effective thermal conductivity and porosity. This hysteresis is more pronounced for the TCR, and relatively smaller for the effective conductivity.

An important finding is the dominant contribution of thermal contact resistance. The ratio of thermal contact to bulk GDL resistance remains approximately constant (2.7/1) over the cyclic compressive load investigated in this work. Also, the effective thermal conductivity increases during unloading due to irreversible deformations occurring during the loading process such as fiber breakage and fiber displacement.

This work has helped clarify the impact of unsteady/cyclic compression on the thermal and structural properties of GDLs and provides new insights on the importance of a key interfacial phenomenon, as well as data that should contribute to further progress in computational fuel cell models.

Acknowledgements

The authors are grateful for the financial support of the Natural Sciences and Engineering Research Council (NSERC) of Canada, and the Canada Research Chairs Program.

References

[1] P. Rama, R. Chen, J. Andrews, J. Power Energy 222 (2008) 421–441.
[2] E. Sadeghi, N. Djilali, M. Bahrami, J. Power Sources (2010), doi:10.1016/j.jpowsour.2010.06.039.
[3] A. Kusoglu, Y. Tang, M.H. Santare, A.M. Karlsson, S. Cleghorn, W.B. Johnson, J. Fuel Cell Sci. Technol. 6 (2009) 011012–011019.
[4] A. Kusoglu, A.M. Karlsson, M.H. Santare, S. Cleghorn, W.B. Johnson, J. Power Sources 161 (2006) 987–996.
[5] J.P. Feser, A.K. Prasad, S.G. Advani, J. Power Sources 162 (2006) 1226–1231.
[6] J. Kleemann, F. Finsterwalder, W. Tillmetz, J. Power Sources 190 (2009) 92–102.
[7] S. Escribano, J.-F. Blachot, J. Etheve, A. Morin, R. Mosdale, J. Power Sources 156 (2006) 8–13.
[8] P. Zhou, C.W. Wu, G.J. Ma, J. Power Sources 159 (2006) 1115–1122.
[9] A. Bazylak, D. Sinton, Z.-S. Liu, N. Djilali, J. Power Sources 163 (2007) 784–792.
[10] I. Nitta, O. Himanen, M. Mikkola, Fuel Cells 08 (2008) 111–119.
[11] O. Burheim, P.J.S. Vi, J.G. Pharoah, S. Kjelstrup, J. Power Sources 195 (2010) 249–256.
[12] M. Khandelwal, M.M. Mench, J. Power Sources 161 (2006) 1106–1115.
[13] C.M. van Wyk, Onderstepoort., J. Vet. Sci. Anim. Ind. 21 (1946) 99–107.
[14] C.M. van Wyk, J. Text. Inst. 37 (1946) T285–T305.
[15] J.I. Dunlop, J. Text. Inst. 74 (1983) 92–97.
[16] I. Krucinska, I. Jalmuzna, W. Zurek, Text. Res. J. 74 (2004) 127–133.
[17] G.A. Carnaby, N. Pan, Text. Res. J. 59 (1989) 275–284.
[18] N.B. Beil, W.W. Roberts, Text. Res. J. 72 (2002) 341–351.
[19] N.B. Beil, W.W. Roberts, Text. Res. J. 72 (2002) 375–382.
[20] S.B. Stankovic, Polym. Eng. Sci. 48 (2008) 676–682.